Discrete stream function method for the incompressible Navier-Stokes equations with simple boundary conditions

Rauan

March 18, 2024

Abstract

The goal of these notes is to present the detailed overview of discrete stream function method for solving incompressible Navier-Stokes equations with simple boundary conditions. We will discuss in detail the scheme formulation, transient and spatial discretizations. After studying these notes one must get a coherent picture of the application of discrete stream function method to incompressible flows and be able to implement the scheme in code.

Contents

1 Introduction

In these notes we will be concerned with the discretization of the Navier-Stokes equations describing the flow of an incompressible fluid:

$$\frac{\partial \boldsymbol{v}}{\partial t} + \boldsymbol{v} \cdot \nabla \boldsymbol{v} = -\nabla p + \epsilon \nabla \cdot \nabla \boldsymbol{v} \tag{1.1a}$$

$$\nabla \cdot \boldsymbol{v} = 0, \tag{1.1b}$$

which are written here in the non-dimensional form, i.e. $\epsilon \equiv Re^{-1}$ for brevity; also $\boldsymbol{v}$ is the velocity and p pressure fields. Since both are necessarily functions of time t and space $\boldsymbol{x}$, their discretization will be denoted by f_i^n, where n is the time level t^n and i is the *mesh* point $\boldsymbol{x}_i$: for example, in the x-direction the interval $x_i < x < x_{i+1}$ is referred to as the *cell* of the mesh. The cell centre corresponds to $x_{i+\frac{1}{2}}$. The mesh points x_i and cell centres $x_{i\pm\frac{1}{2}}$ can be regarded as two overlapping interpenetrating meshes, which together are said to constitute a *staggered* mesh as illustrated in Fig. 1(b). When designing a finite difference or finite volume scheme, we have to choose whether to use the same or different sets of grid points for velocity and pressure. The obvious choice seems to have a single set of points, at which all the variables and all the equations are discretized. Such a grid has the name of a *collocated* or *regular* grid. Albeit simple and easy in operation, the collocated grids were out of favor for a long time because of their tendency to generate spurious oscillations in the solution (cf. §10.2 in [13]) and hence staggered grids are used since the work of Harlow and Welch [6] introducing the marker-and-cell (MAC) method, cf. Fig. 1(a). Colonius [3] uses MAC grid Fig. 1(a), where the indexing uses only integer indices, i.e. $u_{i-\frac{1}{2},j}, v_{i,j-\frac{1}{2}}$ are denoted as $u_{i,j}, v_{i,j}$ and lie on left and bottom sides of cell i, j.

HAVE TO EITHER CHANGE ALL INDICES TO MATCH Fig. 1(b), or change indexation in Fig. 1(b) to match Harlow-Welch [6].

In this paper grid indexation starts at $(x_{\frac{1}{2}}, y_{\frac{1}{2}}) = (0, 0)$ and ends at $(x_{M+\frac{1}{2}}, y_{N+\frac{1}{2}}) = (1, 1)$. The width Δx and height Δy of each cell have the same indexation as the corresponding cells they belong to.

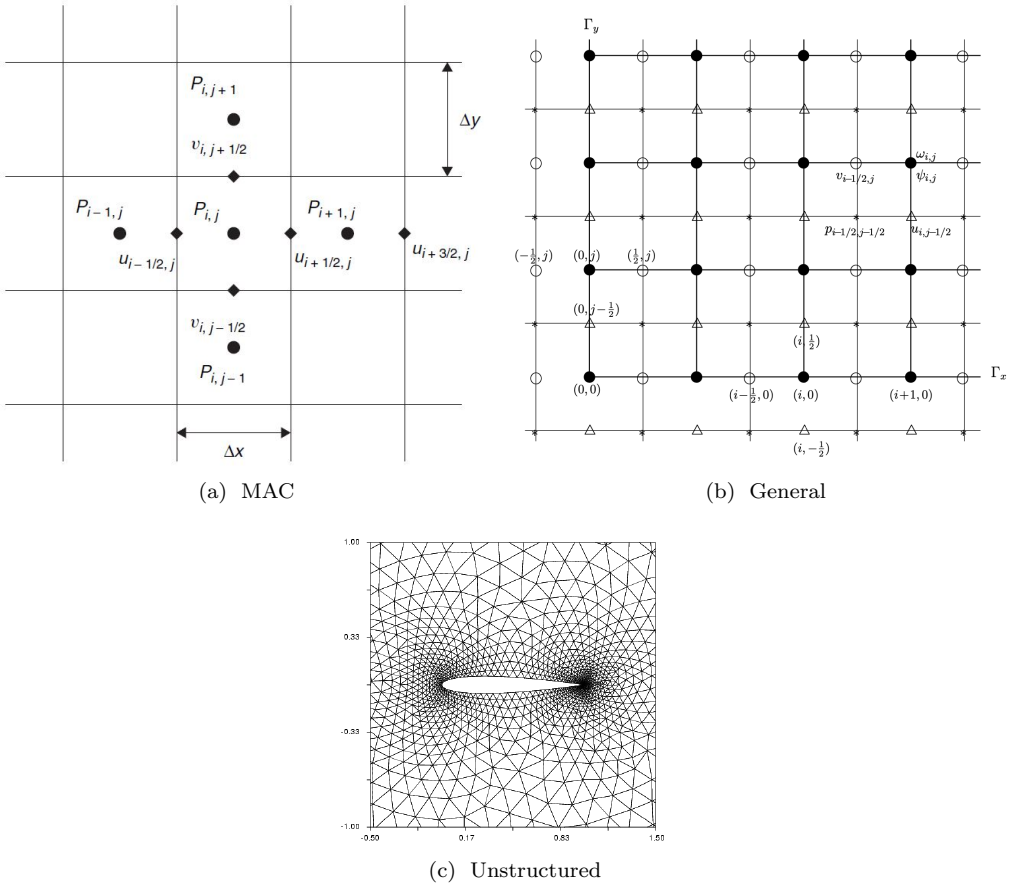

(a) MAC (b) General

(c) Unstructured

Figure 1: Staggered grid.

The staggered arrangement increases complexity of a scheme. Programming becomes more difficult, since it requires accounting for three (u, v, p) or four (u, v, w, p) indexing systems. Interpolations must be used to compute nonlinear terms of momentum equations. Further complications arise when the grid is nonuniform. All these difficulties, however, can be relatively easily handled in computations with structured grids such as those shown in Figs. 1(a) and 1(b). The difficulties of handling a staggered arrangement increase significantly when unstructured (Fig. 1(c)) grids are used. When such grids started to be broadly applied in general-purpose codes in recent years, collocated arrangements returned to favor. This area of CFD is still evolving. We only mention that methods have been developed to cure the splitting problem leading to pressure oscillations, but the cure is not ideal and leads to extra complexities at the implementation level.

In numerical terms, the problem Eqs. (1.1) can be formulated as follows: given the solution p^n, $\boldsymbol{v}^n$ at the previous time layer t^n, find the next time-layer pressure p^{n+1} and velocity $\boldsymbol{v}^{n+1}$ such that they together satisfy the momentum equation, and the velocity is divergence-free $\nabla \cdot \boldsymbol{v}^{n+1} = 0$ and satisfies the boundary conditions.

A conspicuous feature of Eqs. (1.1) is that pressure p is not determined by a time-evolution equation, but rather is implicitly defined by the incompressibility Eq. (1.1b), which plays the role of a constraint that the velocity field $\boldsymbol{v}$ must satisfy. The pressure instantaneously adapts to the evolving velocity field in such a way as to satisfy that constraint. This is reflected in the fact that p satisfies a Poisson equation, which can be derived by taking the divergence of Eq. (1.1a) and combining the result with Eq. (1.1b). From the mathematical viewpoint, this means that the incompressible flow equations have some features of an elliptic system. We can say that the equations are of the mixed hyperbolic (convective terms), parabolic (viscous terms), and elliptic (pressure and incompressibility) type. The elliptic nature of the pressure solution has a physical meaning. It shows that, in an incompressible flow, the pressure field in the entire flow domain adjusts instantaneously to any, however localized, perturbation. This is in perfect agreement with the fact that weak perturbations, for example sound

waves, propagate at infinite speed in incompressible fluids.

Given the Poisson equation for p, it may replace the continuity Eq. (1.1b) and its solution can in principle be substituted back into Eq. (1.1a) to obtain an evolution equation for the velocity field alone. Alternatively, the pressure can be immediately eliminated by taking the curl of momentum Eq. (1.1a), which leads to the vorticity-stream function formulation of incompressible flow. Formal manipulations of this type are useful for various theoretical purposes, but experience has shown that they are rarely advantageous for computational purposes. In most situations, it is preferable to simply approximate and solve Eqs. (1.1) directly for the so-called *primitive* variables $\boldsymbol{v}$ and p.

If, however, one ends up solving the Poisson equation for pressure, an interesting and important question arises as to what boundary conditions should be used for the pressure field. Such conditions are required at every point of the boundary for the Poisson problem to be well-posed. The conditions, however, do not naturally follow from the flow physics for the boundaries between fluid and solid walls, unless, of course, a full fluid-structure interaction problem is solved. Since the latter option is, in most cases, an unnecessary complication, we have to find a way to derive the pressure boundary conditions from the equations themselves.

The remainder of the present paper is organized as follows. In Sections 2 and 3, we describe vorticity-stream function formulation and motivation for numerical scheme. Formulation of the problem in terms of PDE and boundary conditions on a finite domain is performed in Sections 4 to 6. In Sections 7 and 8, we discretize the problem. Boundary conditions are discussed in **??**. Symmetrization of the resulting system of linear equations is performed in Section 9. In Section 10, we discuss the discrete approach to the algorithm, which is finalized in Section 11. The method to obtain a particular solution is described in Section 12. A summary and discussion are given in Section 13.

- ~~Motivation.~~ Added some, where possible!
- ~~BC discussion (analytic).~~ [4, 8, 9, 10, 11, 12].
- ~~Outlet diffusion discretization is problematic. Requested PhD thesis of Jin and Porsillon through UofA library. Wrote an email to their supervisor Prof. Braza and sent a message to Porsillon.~~ Waiting for the response form UofA library since 11th Dec.
- ~~Found this condition $\frac{\partial \boldsymbol{v}}{\partial t} + u\frac{\partial \boldsymbol{v}}{\partial x} + v\frac{\partial \boldsymbol{v}}{\partial y} - \epsilon\frac{\partial^2 \boldsymbol{v}}{\partial y^2} = 0$ by G. Fournier and F. Golanski (2008, but not many citations). They claim Prandtl BL solution for advective bc $\frac{\partial \boldsymbol{v}}{\partial t} + u\frac{\partial \boldsymbol{v}}{\partial x} = 0$ is wrong, while their solution matches Prandtl BL. Looks like we can express the remaining diffusive summand in terms of pressure gradient at the boundary.~~ Wrote an email to author, waiting for the response.
- ~~Change computational domain to inner part only? Boundary values are to be determined by BC, not the momentum eq'n, contrary to Hall~~ [5]. Changed unknowns to inner part only. Values at the boundary are determined using BC.
- ~~Check algebra of diffusion and advection for v component.~~
- It feels like BC scheme which is consistent with inner discretization won't work, we will use Jin-Braza-Braza scheme.
- ~~Outlet BC stated early in non-dim truncated part, but discussion is much later.~~
- Looks like continuous analogue of C^T is determined. Figured out that $C^TC = -L$ and $C^TLC = -L^2$. Some information of transpose of curl is in Vector Calculus notes on page 24 of course by TSOGTGEREL GANTUMUR, but the material is quite heavy. ToDo
- Repeating Fig. 7 from first try of Laplacian and ?? after Artificial BC discussion.
- Paraphrase [1] in Section 11 since most of it is copypaste.
- Boundary conditions for Eq. (3.9) are zero or non-zero.
- Move discrete particular solution Section 12 to the front of algorithm Section 11 and include relationship of particular solution to continuity equation with $\boldsymbol{v} = \boldsymbol{v}_p + \boldsymbol{v}_h$ in prelude to the algorithm Section 3?
- change number of unknowns to include right bdry
- D = -G looks ok, but pressure bc arises
- curl* and curl with bc extra, curl* looks done on paper, indeed a ghost vector arises
- NLBC -> L -> C'C. Here curl* looks to be not equal to C'.
- TOP ABC
- change top boundary condition from SYMMETRY to slip no penetration
- find bc for psi in poisson of stream function.
- Change motivation in symmetrization to normalization.

2 Vorticity-stream function formulation

The algorithm to be used is a combination of classical formulation as in Eqs. (1.1) and vorticity transport equation Eq. (2.4). Consider:

1. Stream function $\psi(x, y, t) : \boldsymbol{v} = \nabla \times \psi$ of an incompressible two-dimensional flow:

$$u = \frac{\partial \psi}{\partial y}, \quad v = -\frac{\partial \psi}{\partial x}, \tag{2.1}$$

   where $\boldsymbol{v} = (u, v)$.

   The velocity vector at every point of space and every moment of time is tangential to the line $\psi = const$ and such lines represent the streamlines of the flow.

2. Vorticity $\omega = \nabla \times \boldsymbol{v}$, in two-dimensional case (x-y-plane) the only non-zero component of ω is z, which leads to

$$\omega = -\frac{\partial u}{\partial y} + \frac{\partial v}{\partial x}. \tag{2.2}$$

Importantly, continuity Eq. (1.1b) is satisfied immediately by taking spatial derivatives of stream function Eq. (2.1) components and adding them up. The governing Eqs. (1.1) can now be transformed. The new equations are changed to the following:

1. Transport equation for vorticity.

   Application of $(\nabla\times)$ to momentum and taking into account continuity Eq. (1.1b) together with the fact

$$\frac{\partial}{\partial y}\left(\frac{\partial p}{\partial x}\right) - \frac{\partial}{\partial x}\left(\frac{\partial p}{\partial y}\right) = 0 \tag{2.3}$$

   results in

$$\boxed{\frac{\partial \omega}{\partial t} - \epsilon\left(\frac{\partial^2 \omega}{\partial x^2} + \frac{\partial^2 \omega}{\partial y^2}\right) = -\left(u\frac{\partial \omega}{\partial x} + v\frac{\partial \omega}{\partial y}\right),} \tag{2.4}$$

   where we moved advection terms to the right hand side with intent to linearize them later.

2. Vorticity-Stream function equation.

   After substituting stream function Eq. (2.1) into vorticity Eq. (2.2) we obtain

$$\boxed{\nabla^2 \psi = -\omega.} \tag{2.5}$$

These two equations above form a coupled system, and the pressure field does not explicitly appear in neither Eq. (2.4) nor Eq. (2.5) and, in principle, is not needed in the solution.

The system (Eqs. (2.4) and (2.5)) requires boundary conditions on ψ and ω. For the stream function, imposing physically plausible conditions is not difficult. One has to write the proper boundary conditions for the velocity components and use the definition of Eq. (2.1) to represent them as conditions for ψ. Values for ψ and its derivatives are obtained by integrating Eq. (2.1). For instance, in case of vertical boundary

$$1 = u = \frac{\partial \psi}{\partial y} \implies \frac{\partial \psi}{\partial y} = 1 \implies \psi_1(t, y) = a_1 y + a_2 + \psi_2(t, x), \tag{2.6}$$

$$0 = v = -\frac{\partial \psi}{\partial x} \implies \psi = \psi_1(t, y) + a_3 \text{ (can be made compatible with other BCs)}, \tag{2.7}$$

where a_1, a_2, a_3 are constants. The situation is more difficult in the case of vorticity. There are no natural boundary conditions on ω, but they can be derived from the conditions on ψ by application of Eq. (2.5) at the boundary. The process of finding boundary conditions of ω typically results in expressions containing second derivatives, therefore, special numerical treatment is required.

3 Prelude to the algorithm using continuous operators

We now modify momentum Eq. (1.1a) in 2D in a similar manner as in Section 2 with a help of differential operators. These operators can be transformed into discrete format without much difficulties. Hence, we can apply the similar process to system of linear equations generated by Eq. (1.1a) by multiplying it with the corresponding matrices, which is discussed in Sections 10 and 11.

Define

$$\operatorname{curl} = \begin{bmatrix} \frac{\partial}{\partial y} \\ -\frac{\partial}{\partial x} \end{bmatrix}. \tag{3.1}$$

Hence, by stream function Eq. (2.1) we have $\boldsymbol{v} = \operatorname{curl} \psi$. Lastly, define

$$\operatorname{curl}^* = \begin{bmatrix} -\frac{\partial}{\partial y} & \frac{\partial}{\partial x} \end{bmatrix}. \tag{3.2}$$

Let us now compute curl^* applied to velocity vector $\boldsymbol{v}$

$$\operatorname{curl}^* \boldsymbol{v} = \operatorname{curl}^* \operatorname{curl} \psi = \begin{bmatrix} -\frac{\partial}{\partial y} & \frac{\partial}{\partial x} \end{bmatrix} \begin{bmatrix} \frac{\partial}{\partial y} \\ -\frac{\partial}{\partial x} \end{bmatrix} \psi = \left(-\frac{\partial^2}{\partial y^2} - \frac{\partial^2}{\partial x^2} \right) \psi = -\nabla^2 \psi. \tag{3.3}$$

By taking into account commutativity of partial derivatives with respect to time and space we obtain

$$\operatorname{curl}^* \left(\frac{\partial}{\partial t} \right) \operatorname{curl} \psi = -\frac{\partial}{\partial t} \left(\nabla^2 \psi \right). \tag{3.4}$$

Applying curl^* to Laplacian of velocity leads to

$$\begin{aligned} \operatorname{curl}^* \nabla^2 \boldsymbol{v} &= \operatorname{curl}^* \nabla^2 \operatorname{curl} \psi \\ &= \begin{bmatrix} \frac{\partial}{\partial y} & -\frac{\partial}{\partial x} \end{bmatrix} \begin{bmatrix} \frac{\partial^2}{\partial x^2} + \frac{\partial^2}{\partial y^2} & 0 \\ 0 & \frac{\partial^2}{\partial x^2} + \frac{\partial^2}{\partial y^2} \end{bmatrix} \begin{bmatrix} -\frac{\partial}{\partial y} \\ \frac{\partial}{\partial x} \end{bmatrix} \psi \\ &= \begin{bmatrix} \frac{\partial}{\partial y} \left(\frac{\partial^2}{\partial x^2} + \frac{\partial^2}{\partial y^2} \right) & 0 \\ 0 & -\frac{\partial}{\partial x} \left(\frac{\partial^2}{\partial x^2} + \frac{\partial^2}{\partial y^2} \right) \end{bmatrix} \begin{bmatrix} -\frac{\partial}{\partial y} \\ \frac{\partial}{\partial x} \end{bmatrix} \psi \\ &= -\nabla^2 \left(\nabla^2 \psi \right). \end{aligned} \tag{3.5}$$

Our goal is to obtain equation in terms of ψ by modifying Eq. (1.1a). The procedure lies in transforming this equation into vorticity transport Eq. (2.4) with the help of vorticity stream function substitution Eq. (2.5) and curl, curl^* operators. Firstly, we put transient, gradient and viscous terms to the left hand side, whereas non-linear terms are linearized and moved to the right. Next, we substitute $\boldsymbol{v} = \operatorname{curl} \boldsymbol{\psi}$ and apply curl^* to rearranged momentum Eq. (1.1a), which eliminates the pressure gradient ($\operatorname{curl}^* \operatorname{grad} = \begin{bmatrix} -\frac{\partial}{\partial y} & \frac{\partial}{\partial x} \end{bmatrix} \begin{bmatrix} \frac{\partial}{\partial x} \\ \frac{\partial}{\partial y} \end{bmatrix} = 0$). For 2-dimensional case from Eqs. (3.4) and (3.5) , we get

$$\operatorname{curl}^* \left(\frac{\partial \boldsymbol{v}}{\partial t} - \epsilon \nabla^2 \boldsymbol{v} \right) = \operatorname{curl}^* \left(\boldsymbol{v} \cdot \nabla \boldsymbol{v} \right) \tag{3.6}$$

$$\operatorname{curl}^* \left(\frac{\partial}{\partial t} \operatorname{curl} \psi - \epsilon \nabla^2 \operatorname{curl} \psi \right) = \operatorname{curl}^* \left(\boldsymbol{v} \cdot \nabla \boldsymbol{v} \right) \tag{3.7}$$

$$\left(\frac{\partial}{\partial t} - \epsilon \nabla^2 \right) \left(-\nabla^2 \psi \right) = \operatorname{curl}^* \left(\boldsymbol{v} \cdot \nabla \boldsymbol{v} \right) \tag{3.8}$$

Solving Eq. (3.8) for $\nabla^2 \psi$ is equivalent to obtaining solution for Poisson Eq. (2.5). However, we can go through Eq. (3.8) and solve it in one step by obtaining ψ from biharmonic equation

$$\boxed{-\frac{\partial \nabla^2 \psi}{\partial t} + \epsilon \nabla^4 \psi = \operatorname{curl}^* \left(\boldsymbol{v} \cdot \nabla \boldsymbol{v} \right),} \tag{3.9}$$

where the right hand side contains boundary conditions (in numerical sense) and non-linear advective terms, which were initially stated in terms of $\boldsymbol{v}, p$ and transformed through premultiplication by curl^T.

Assume that the general solution to Eqs. (1.1) is represented as a sum of homogeneous and inhomogeneous velocity vector fields

$$\boldsymbol{v} = \boldsymbol{v}_h + \boldsymbol{v}_p, \tag{3.10}$$

where $\boldsymbol{v}_h$ satisfies momentum Eq. (1.1a) with homogeneous continuity $\nabla \cdot \boldsymbol{v}_h = 0$, whereas the particular solution is obtained from $\nabla \cdot \boldsymbol{v}_p = \hat{bc}_2$. We will discuss the numerical details of this approach in Sections 8 and 11. Vector field $\boldsymbol{v}_h$ considers the solution of biharmonic Eq. (3.9) for ψ vanishing at the boundary $\partial\Omega$, which matches the numerical computations of the Laplacian operator for ψ in Section 10. Eq. (3.9) is solved for ψ using the zero boundary conditions **(LOOKS LIKE NONZERO, BUT PURE DIRICHLET, CHECKING THE CODE NOW)**, whereas the particular solution $\boldsymbol{v}_p$ is obtained from $\nabla \cdot \boldsymbol{v}_p = \hat{bc}_2$ with non-zero boundary conditions. Finally, we arrive to the general solution of system of Eqs. (1.1)

$$\boxed{\boldsymbol{v} = \boldsymbol{v}_p + \operatorname{curl} \psi.} \tag{3.11}$$

3.1 Vector fields that vanish at the boundary

This subsection contains side notes for Section 3, here we discuss some properties of differential operators in vector calculus. Consider continuous operators div, curl and grad on bounded domain Ω with boundary $\partial\Omega$. Let all vector $\boldsymbol{X}, \boldsymbol{Y}$ and scalar ϕ, ψ fields vanish at $\partial\Omega$. Denote by SF the set of all scalar fields in Ω, and by VF the set of all vector fields in Ω. In this subsection we need to have inner products in inner product space [1]. Define scalar and vector inner products as

$$\langle \phi, \psi \rangle = \int_\Omega \phi\psi \; dV, \quad \langle \boldsymbol{X}, \boldsymbol{Y} \rangle = \int_\Omega \boldsymbol{X} \cdot \boldsymbol{Y} \; dV. \tag{3.12}$$

Then define the transpose of grad as an operator $\operatorname{grad}^T : VF \to SF$ such that

$$\langle \operatorname{grad} \phi, \boldsymbol{X} \rangle = \left\langle \phi, \operatorname{grad}^T \boldsymbol{X} \right\rangle, \tag{3.13}$$

for all vector fields $\boldsymbol{X}$ and scalar fields ϕ vanishing at the boundary $\partial\Omega$. To identify this operator, integrate the identity

$$\nabla \cdot (\phi \boldsymbol{X}) = \nabla\phi \cdot \boldsymbol{X} + \phi \nabla \cdot \boldsymbol{X}, \tag{3.14}$$

and apply the divergence theorem, to get

$$\int_{\partial\Omega} \phi \boldsymbol{X} \cdot \boldsymbol{n} \; dS = \int_\Omega \nabla \cdot (\phi \boldsymbol{X}) \; dV = \int_\Omega \nabla\phi \cdot \boldsymbol{X} \; dV + \int_\Omega \phi \nabla \cdot \boldsymbol{X} \; dV. \tag{3.15}$$

Since $\phi = 0$ on $\partial\Omega$, left side of Eq. (3.15) vanishes. Hence, we infer

$$0 = \langle \nabla\phi, \boldsymbol{X} \rangle + \langle \phi, \nabla \cdot \boldsymbol{X} \rangle, \tag{3.16}$$

implying that the transpose of the gradient is the negative divergence, and the transpose of the divergence is the negative gradient:

$$\operatorname{grad}^T = -\operatorname{div}, \qquad \operatorname{div}^T = -\operatorname{grad}. \tag{3.17}$$

We now move to 3-dimensional case, consider the following identity

$$\nabla \cdot (\boldsymbol{X} \times \boldsymbol{Y}) = (\nabla \times \boldsymbol{X}) \cdot \boldsymbol{Y} - \boldsymbol{X} \cdot (\nabla \times \boldsymbol{Y}). \tag{3.18}$$

Navier-Stokes Eqs. (1.1) are defined in the whole domain from $-\infty$ to $+\infty$ in each axis. In our problem and operators $\operatorname{curl}, \operatorname{grad}, \operatorname{div}$ are local. Therefore, we are allowed to let velocity vector fields vanish at the boundaries $\pm\infty$. Since we consider only those vector fields that go to zero at $\partial\Omega$, divergence theorem yields

$$\begin{aligned} 0 = \int_{\partial\Omega} (\boldsymbol{X} \times \boldsymbol{Y}) \cdot \boldsymbol{n} \; dS = \int_\Omega \nabla \cdot (\boldsymbol{X} \times \boldsymbol{Y}) \; dV = \\ = \int_\Omega (\nabla \times \boldsymbol{X}) \cdot \boldsymbol{Y} \; dV - \int_\Omega \boldsymbol{X} \cdot (\nabla \times \boldsymbol{Y}) \; dV = \langle \operatorname{curl} \boldsymbol{X}, \boldsymbol{Y} \rangle - \langle \boldsymbol{X}, \operatorname{curl}^T \boldsymbol{Y} \rangle, \end{aligned} \tag{3.19}$$

which identifies the curl as the transpose of itself in 3D:

$$\operatorname{curl}^T = \operatorname{curl}. \tag{3.20}$$

4 Problem statement

Let the velocity vector $\boldsymbol{v}(t,x,y) = (u(t,x,y), v(t,x,y))$ and pressure $p(t,x,y)$ be the solutions to Eqs. (1.1) on in rectangular domain $\Omega : 0 \le x < L, 0 \le y < H$ together with boundary conditions on $\partial\Omega$:

$$\text{Momentum: } \frac{\partial \boldsymbol{v}}{\partial t} + \boldsymbol{v}\cdot\nabla\boldsymbol{v} = -\frac{1}{\rho}\nabla p + \frac{\mu}{\rho}\nabla\cdot\nabla\boldsymbol{v} \quad \text{in } \Omega, \tag{4.1a}$$

ρ - density, μ - dynamic viscosity.

$$\text{Continuity: } \nabla\cdot\boldsymbol{v} = 0 \quad \text{in } \Omega, \tag{4.1b}$$

$$\text{Normal BC: } \boldsymbol{v}(t,x,y)\cdot\hat{\mathbf{n}} = \boldsymbol{v}_{\hat{\mathbf{n}}}(t,x,y) \quad \text{on } \partial\Omega, \tag{4.1c}$$

$$\text{Tangential BC: } \boldsymbol{v}(t,x,y)\cdot\hat{\mathbf{t}} = \boldsymbol{v}_{\hat{\mathbf{t}}}(t,x,y) \quad \text{on } \partial\Omega, \tag{4.1d}$$

$$\text{Initial condition: } \boldsymbol{v}(0,x,y) = g(x,y) \quad \text{in } \Omega, \tag{4.1e}$$

where $\hat{\mathbf{n}}, \hat{\mathbf{t}}$ are normal and tangential unit vectors to the $\partial\Omega$ boundary.

5 Nondimensionalization

In numerical computations, it is advantageous to maintain variables of comparable magnitude. This ensures that operations such as the multiplication of a large dimensional pressure variable with a small velocity are not performed.

We will truncate the domain and normalize all equations by width L and maximum velocity at the boundary U_0. After introducing the following dimensionless variables (marked with prime $'$):

$$x \to Lx', \quad \boldsymbol{v} \to U_0\boldsymbol{v}', \quad \nabla \to \frac{1}{L}\nabla', \quad p \to p'\rho U_0^2, \quad t \to \frac{L}{U_0}t',$$

we obtain

$$\frac{U_0}{\frac{L}{U_0}}\frac{\partial \boldsymbol{v}'}{\partial t'} + U_0\boldsymbol{v}\cdot\left(\frac{1}{L}\nabla'\right)U_0\boldsymbol{v} = -\frac{1}{\rho}\left(\frac{1}{L}\nabla'\right)p'\rho U_0^2 + \frac{\mu}{\rho}\left(\frac{1}{L}\nabla'\right)\cdot\left(\frac{1}{L}\nabla'\right)U_0\boldsymbol{v}'.$$

After multiplying both sides of the equation by $\frac{L}{U_0^2}$ and introducing well-known Reynolds number

$$\mathrm{Re} = \frac{\rho L U_0}{\mu},$$

we obtain the non-dimensional momentum equation

$$\frac{\partial \boldsymbol{v}}{\partial t} + \boldsymbol{v}\cdot\nabla\boldsymbol{v} = -\nabla p + \frac{1}{\mathrm{Re}}\nabla\cdot\nabla\boldsymbol{v},$$

where prime superscript $'$ is suppressed for the dimensionless variables. The continuity equation is nondimensionalized in a similar manner:

$$\left(\frac{1}{L}\nabla'\right)\cdot U_0\boldsymbol{v}' = 0 \iff \nabla'\cdot\boldsymbol{v}' = 0 \implies \nabla\cdot\boldsymbol{v} = 0,$$

where we drop prime superscripts in the last identity as well.

6 Problem statement on truncated domain

The initial Eqs. (4.1) from Section 4 on semi-infinite domain now become a system of partial differential equations on a unit square domain

$$\text{Momentum: } \frac{\partial \boldsymbol{v}}{\partial t} + \boldsymbol{v} \cdot \nabla \boldsymbol{v} = -\nabla p + \epsilon \nabla \cdot \nabla \boldsymbol{v} \qquad \text{in } \Omega, \tag{6.1a}$$

$$\epsilon = \frac{1}{\mathrm{Re}}, 0 \le x \le 1, 0 \le y \le 1, t \ge 0.$$

$$\text{Continuity: } \nabla \cdot \boldsymbol{v} = 0 \qquad \text{in } \Omega, \tag{6.1b}$$

$$0 \le x \le 1, 0 \le y \le 1, t \ge 0.$$

$$\text{Normal BC: } \boldsymbol{v}(t,x,y) \cdot \hat{\mathbf{n}} = \boldsymbol{v}_{\hat{\mathbf{n}}}(t,x,y) \qquad \text{on } \partial\Omega, \tag{6.1c}$$

$$\text{Tangential BC: } \boldsymbol{v}(t,x,y) \cdot \hat{\mathbf{t}} = \boldsymbol{v}_{\hat{\mathbf{t}}}(t,x,y) \qquad \text{on } \partial\Omega, \tag{6.1d}$$

$$\text{Initial condition: } \boldsymbol{v}(0,x,y) = g(x,y) \qquad \text{in } \Omega, \tag{6.1e}$$

7 Domain discretization

Following the nondimensionalization of the governing equations, we now turn our attention to the process of domain discretization. This crucial step involves dividing the computational domain into discrete elements, allowing us to compute variables and their derivatives on a finite set of points called grid. Consider discretizing the area into M intervals horizontally and N intervals vertically forming a mesh of rectangular cells. To enhance memory access it is recommended to organize the data using vectors instead of matrices. The reason behind is memory access time; a single index i works faster than double i, j in most programming languages. In this section, however, for the sake of simplicity, we use two indices i, j (column and row as in Harlow and Welch [6]) to represent coordinates on the grid.

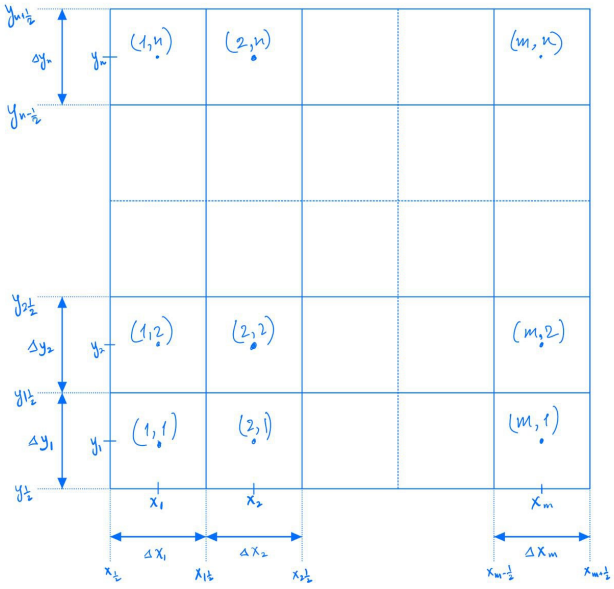

Figure 2: Domain discretization (here $m = M, n = N$)

To eliminate the necessity of solving an additional equation for pressure we will be using a staggered grid arrangement. Details are discussed in Sections 8.3, 8.4 and 10. Moreover, the pressure gradients can be evaluated directly using central differences on such grids. This calculation on staggered grids does not require any interpolation, furthermore, it is computationally cheaper and simpler to implement.

The u velocity components are stored at the centres of vertically oriented faces, while the values of v are stored at the centres of horizontal ones. The number of unknown components inside the domain (excluding boundaries) is $M(N-1)$ for v and $(M-1)N$ for u. At the line (row) with coordinate y_1 there are $M-1$ unknown u components located inside the domain with a total of N such y horizontal lines.

In **??**, the values of u for the outlet are not explicitly defined. To address this, we will express the values on the boundary using **??** in terms of data from inner part of the domain. These arrays for u and v are then concatenated into a single vector $\boldsymbol{v}$ of size $M(N-1)+(M-1)N$.

Increasing the accuracy closer to the wall and the outlet does look advantageous, hence, we will refine the grid using the standard ratio rule $\Delta x_{i+1} = k_x \Delta x_i, \Delta y_{j+1} = k_y \Delta y_j$ with constants k_x, k_y close to the value of 1.

8 Discrete operators

This subsection focuses on the specific operators used in the discretization of Eqs. (6.1), providing the mathematical tools necessary to transform these continuous equations into a form that can be solved numerically.

Denote discrete spatial operators as:

$\hat{L}$: Laplacian.

$\hat{G}$: Gradient.

$\hat{D}$: Divergence.

$\hat{\mathbf{H}}$: Non-linear advective terms.

Then initial system of Eqs. (6.1) can be approximated using such operators as

$$\begin{bmatrix} \mathbf{I} & 0 \\ 0 & 0 \end{bmatrix} \frac{\partial}{\partial t} \begin{pmatrix} \boldsymbol{v} \\ p \end{pmatrix} = \begin{bmatrix} \hat{L} & -\hat{G} \\ -\hat{D} & 0 \end{bmatrix} \begin{bmatrix} \boldsymbol{v} \\ p \end{bmatrix} + \begin{pmatrix} -\hat{\mathbf{H}}(\boldsymbol{v}) \\ 0 \end{pmatrix} + \mathrm{bc}_{\boldsymbol{v},p}, \tag{8.1}$$

where boundary conditions are in terms of pressure and velocity. In the following subsections, each of the discrete operators is described individually.

Attack Sys. (8.1) with the following schemes as in Colonius [3] (superscript denotes the time step):

Viscous - Implicit trapezoidal - Crank Nicholson scheme (second-order method in time).

$$\hat{L}\boldsymbol{v} = \frac{1}{2}\left(\hat{L}\boldsymbol{v}^{n+1} + \hat{L}\boldsymbol{v}^{n}\right) \tag{8.2}$$

Nonlinear - Explicit Adams-Bashforth (second-order method in time).

$$\hat{\mathbf{H}}(\boldsymbol{v}) = \frac{3}{2}\hat{\mathbf{H}}(\boldsymbol{v}^{n}) - \frac{1}{2}\hat{\mathbf{H}}(\boldsymbol{v})^{n-1}. \tag{8.3}$$

Pressure - Implicit Euler, though the pressure variable will be later eliminated in the algorithm (first-order method in time).

$$\hat{G}p = \hat{G}p^{n+1}. \tag{8.4}$$

The above schemes result in the following time-discretized system:

$$\begin{bmatrix} \frac{1}{\Delta t}\mathbf{I} - \frac{1}{2}\hat{L} & \hat{G} \\ \hat{D} & 0 \end{bmatrix} \begin{pmatrix} \boldsymbol{v}^{n+1} \\ p^{n+1} \end{pmatrix} = \begin{pmatrix} \left[\frac{1}{\Delta t}\mathbf{I} - \frac{1}{2}\hat{L}\right]\boldsymbol{v}^{n} - \left[\frac{3}{2}\hat{\mathbf{H}}(\boldsymbol{v}^{n}) - \frac{1}{2}\hat{\mathbf{H}}(\boldsymbol{v}^{n-1})\right] \\ 0 \end{pmatrix} + \begin{pmatrix} \hat{bc}_1 \\ \hat{bc}_2 \end{pmatrix} \tag{8.5}$$

and **??**

$$\begin{aligned} \frac{\boldsymbol{v}^{n+1} - \boldsymbol{v}^{n}}{\Delta t} + \left[\frac{3}{2}u^{n}\left(\frac{\partial \boldsymbol{v}}{\partial x}\right)^{n} - \frac{1}{2}u^{n-1}\left(\frac{\partial \boldsymbol{v}}{\partial x}\right)^{n-1}\right] \\ = \epsilon\left[\left(\frac{\partial^2 \boldsymbol{v}}{\partial y^2}\right)^{n+1} + \left(\frac{\partial^2 \boldsymbol{v}}{\partial y^2}\right)^{n}\right], \end{aligned} \tag{8.6}$$

however, the results produced with such BC (8.6) schemes are yet to be known and should be compared with BC (8.7) from the corresponding paper of Jin-Braza [7], which was said to be

$$\begin{aligned} \frac{\boldsymbol{v}^{n+1} - \boldsymbol{v}^{n}}{\Delta t} + \frac{u^{n}}{2}\left[\left(\frac{\partial \boldsymbol{v}}{\partial x}\right)^{n+1} + \left(\frac{\partial \boldsymbol{v}}{\partial x}\right)^{n}\right] \\ = \epsilon\left(\frac{\partial^2 \boldsymbol{v}}{\partial y^2}\right)^{n}. \end{aligned} \tag{8.7}$$

We will first use discretized BC (8.7) from Jin-Braza [7] as it was shown to be stable and produced solid results. Later on we can proceed with discretized BC (8.6) which is consistent with our schemes after developing the necessary techniques.

After applying the discrete operators listed in the following Sections 8.1 to 8.4, we rewrite Sys. (8.5) as

$$\boxed{\begin{bmatrix} \hat{A} & \hat{G} \\ \hat{D} & 0 \end{bmatrix} \begin{pmatrix} \boldsymbol{v}^{n+1} \\ p^{n+1} \end{pmatrix} = \begin{pmatrix} \hat{r}^n \\ 0 \end{pmatrix} + \begin{pmatrix} \hat{bc}_1 \\ \hat{bc}_2 \end{pmatrix},} \tag{8.8}$$

where $\hat{r}^n$ includes viscous, non-linear and gradient terms from time steps $n, n-1$ and $\hat{bc}_i$ are explicit boundary values in terms of velocity and pressure.

8.1 Laplacian

As per Sys. (8.5) it is required to approximate implicit viscous terms spatially. In order to obtain the discrete operator acting on a velocity vector we will rewrite Laplacian as a block matrix:

$$\hat{L} = \begin{bmatrix} \hat{L}^u_{xx} + \hat{L}^u_{yy} & 0 \\ 0 & \hat{L}^v_{xx} + \hat{L}^v_{yy} \end{bmatrix}.$$

Each pair of the matrices $\hat{L}^u_{xx}, \hat{L}^v_{xx}$ and $\hat{L}^u_{yy}, \hat{L}^v_{yy}$ will be equal on a uniform, but different on non-uniform grids. These matrices are computed similarly. Below we will discuss how the Laplacian matrix is constructed at different parts of the grid.

8.1.1 Inner part

The uniform grid refinement $\Delta x_{i+1} = k_x \Delta x_i, \Delta y_{j+1} = k_y \Delta y_j$ makes the order of the scheme consistent throughout the whole domain. Without loss of generality, let us show how to compute $\hat{L}^u_{xx}$. The other three matrices can be constructed in a similar manner. The power series of of $u_{i-\frac{1}{2}\pm 1,j}$ at nodes $x_{i-\frac{1}{2}\pm 1}$ with respect to $u_{i-\frac{1}{2},j}$ at node $x_{i-\frac{1}{2}}$ are

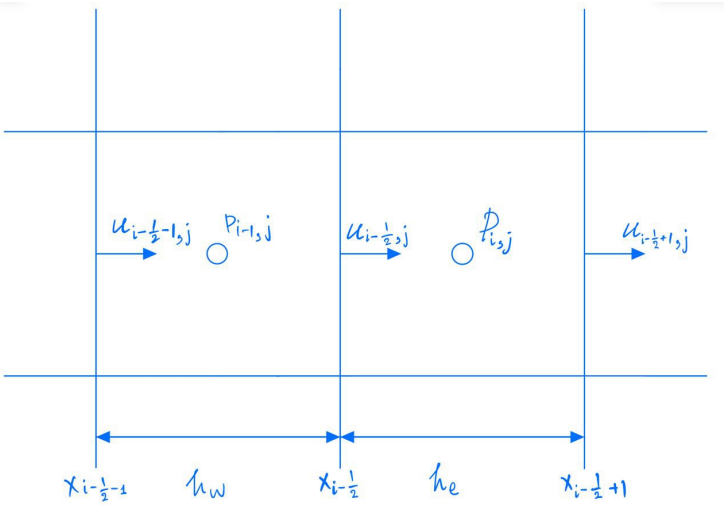

Figure 3: $\hat{L}^u_{xx}$ inner part.

$$u_{i-\frac{1}{2}+1,j} = u_{i-\frac{1}{2},j} + \left.\frac{\partial u}{\partial x}\right|_{i-\frac{1}{2},j} \left(x_{i-\frac{1}{2}+1} - x_{i-\frac{1}{2}}\right) + \frac{1}{2} \left.\frac{\partial^2 u}{\partial x^2}\right|_{i-\frac{1}{2},j} \left(x_{i-\frac{1}{2}+1} - x_{i-\frac{1}{2}}\right)^2 + O\left(\Delta x^3\right), \tag{8.9}$$

$$u_{i-\frac{1}{2}-1,j} = u_{i-\frac{1}{2},j} + \left.\frac{\partial u}{\partial x}\right|_{i-\frac{1}{2},j} \left(x_{i-\frac{1}{2}-1} - x_{i-\frac{1}{2}}\right) + \frac{1}{2} \left.\frac{\partial^2 u}{\partial x^2}\right|_{i-\frac{1}{2},j} \left(x_{i-\frac{1}{2}-1} - x_{i-\frac{1}{2}}\right)^2 + O\left(\Delta x^3\right). \tag{8.10}$$

We can combine Eqs. (8.9) and (8.10) by cancelling the first derivative, which will result in

$$\left.\frac{\partial^2 u}{\partial x^2}\right|_{i-\frac{1}{2},j} \approx \frac{u_{i-\frac{1}{2}+1,j}\left(x_{i-\frac{1}{2}} - x_{i-\frac{1}{2}-1}\right) - u_{i-\frac{1}{2},j}\left(x_{i-\frac{1}{2}+1} - x_{i-\frac{1}{2}-1}\right) + u_{i-\frac{1}{2}-1,j}\left(x_{i-\frac{1}{2}+1} - x_{i-\frac{1}{2}}\right)}{\left(\frac{x_{i-\frac{1}{2}+1} - x_{i-\frac{1}{2}-1}}{2}\right)\left(x_{i-\frac{1}{2}} - x_{i-\frac{1}{2}-1}\right)\left(x_{i-\frac{1}{2}+1} - x_{i-\frac{1}{2}}\right)} + O(\Delta x)$$

$$\approx \frac{1}{h_c h_e} u_{i-\frac{1}{2}+1,j} - \frac{2}{h_w h_e} u_{i-\frac{1}{2},j} + \frac{1}{h_c h_w} u_{i-\frac{1}{2}-1,j} + O(\Delta x), \tag{8.11}$$

where $h_w = x_{i-\frac{1}{2}} - x_{i-\frac{1}{2}-1}, h_c = \frac{x_{i-\frac{1}{2}+1} - x_{i-\frac{1}{2}-1}}{2}, h_e = x_{i-\frac{1}{2}+1} - x_{i-\frac{1}{2}}$ as in Fig. 3. The coefficients in front of the velocity components are then placed into the $\hat{L}^u_{xx}$ matrix. The order of this approximation becomes 2^{nd} for uniform grids.

8.1.2 Normal velocity to the boundary

The exact value of the normal velocity to the boundary ($u_{\frac{1}{2},j}$ on Fig. 4) is given as a Dirichlet boundary condition, hence, it is possible to move the corresponding terms together with the coefficients to the right-hand side of the linear system and treat the values explicitly. The values are moved to the vector $\hat{bc}_1$ on the right-hand side of Sys. (8.5).

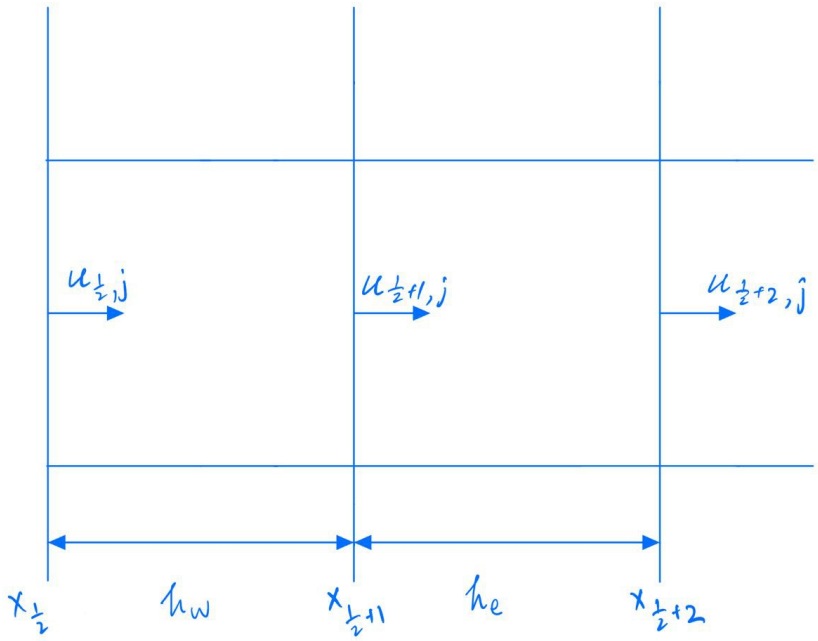

Figure 4: $\hat{L}^u_{xx}$ at the left boundary.

In this particular case on the left side of the domain we have

$$\left.\frac{\partial^2 u}{\partial x^2}\right|_{\frac{1}{2}+1,j} \approx \frac{1}{h_c h_e} u_{\frac{1}{2}+2,j} - \frac{2}{h_w h_e} u_{\frac{1}{2}+1,j} + \frac{1}{h_c h_w} u_{\frac{1}{2},j} + O(\Delta x), \tag{8.12}$$

$$\approx \frac{1}{h_c h_e} u_{\frac{1}{2}+2,j} - \frac{2}{h_w h_e} u_{\frac{1}{2}+1,j} + \frac{1}{h_c h_w} \boldsymbol{v}_{\hat{\mathbf{n}}}(t,x,y) + O(\Delta x), \tag{8.13}$$

$$\tag{8.14}$$

then for the corresponding row of a linear system we get

$$\frac{1}{h_c h_e} u_{\frac{1}{2}+2,j} - \frac{2}{h_w h_e} u_{\frac{1}{2}+1,j} = -\frac{1}{h_c h_w} \boldsymbol{v}_{\hat{\mathbf{n}}}(t,x,y), \tag{8.15}$$

where the left side contains unknowns to be solved for, and the right hand side contains explicit boundary condition.

8.1.3 Tangential velocity at the boundary

Most of the flow that differs much from the freestream is likely to happen closer to the wall, thus, we can incorporate symmetric boundary conditions over the top. **??** leads to $v_{\text{top}} = 0, u_{\text{top}} = u_{\text{freestream}}$, which affects only the $\hat{L}^u_{yy}$ and $\hat{L}^v_{yy}$ due to the 5-point stencil discretization. We will focus on $\hat{L}^u_{yy}$ in this part; $\hat{L}^v_{yy}$ is computed in a similar manner. The resultant contribution to the corresponding linear equation from Laplace operator

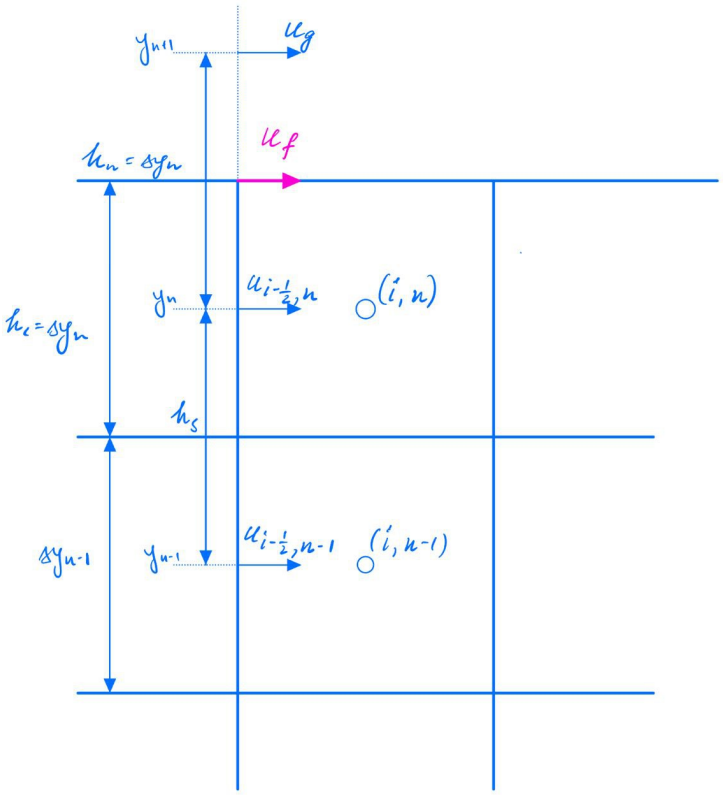

Figure 5: $\hat{L}^u_{yy}$ at top boundary.

Consider the neighbouring cells near the wall as in Fig. 5. Resultant Eq. (8.12) can be written as

$$\left.\frac{\partial^2 u}{\partial y^2}\right|_{i-\frac{1}{2},N} = \frac{u_g\,(h_s) + u_{i-\frac{1}{2},N}\,(-2h_c) + u_{i-\frac{1}{2},N-1}\,(h_n)}{h_n h_s h_c}, \tag{8.16}$$

where $h_s = y_n - y_{n-1}, h_n = y_{n+1} - y_n, h_c = \frac{y_{n+1}-y_{n-1}}{2} = \frac{h_s+h_n}{2}$.

It is possible to make the order of the scheme $O(\Delta y^2)$ near the boundary as per Eq. (8.12) if u_g and $u_{i-\frac{1}{2},N-1}$ are set to be equidistant from $u_{i-\frac{1}{2},N}$.The value of u along the top face is known to be freestream velocity u_f, interpolation of freestream velocity $u_f = \frac{u_g + u_{i-\frac{1}{2},N}}{2} \implies u_g = 2u_f - u_{i-\frac{1}{2},N}$, which we can plug into Eq. (8.16) from above to obtain

$$\begin{aligned}
\left.\frac{\partial^2 u}{\partial y^2}\right|_{i-\frac{1}{2},N} &= \frac{2u_f h_s}{h_n h_s h_c} + u_{i-\frac{1}{2},N}\left(\frac{-h_s}{h_n h_s h_c} + \frac{-2h_c}{h_n h_s h_c}\right) + u_{i-\frac{1}{2},N-1}\frac{h_n}{u_c h_s h}, \\
\left.\frac{\partial^2 u}{\partial y^2}\right|_{i-\frac{1}{2},N} &= \frac{2u_f}{h_c h_c} + u_{i-\frac{1}{2},N}\left(\frac{-(2h_c+h_s)}{h_c h_s h_c}\right) + u_{i-\frac{1}{2},N-1}\frac{1}{h_s h_c}, \\
\left.\frac{\partial^2 u}{\partial y^2}\right|_{i-\frac{1}{2},N} &= \frac{2u_f}{{h_c}^2} + u_{i-\frac{1}{2},N}\left(\frac{-(2h_c+h_s)}{h_c^2 h_s}\right) + u_{i-\frac{1}{2},N-1}\frac{1}{h_s h_c}.
\end{aligned} \tag{8.17}$$

The first summand from the above equation is treated explicitly, i.e. moved to the vector $\hat{bc}_1$ on the right-hand side in Sys. (8.5), while the other two coefficients are used as elements for the $\hat{L}^u_{yy}$ matrix.

8.1.4 Bottom boundary

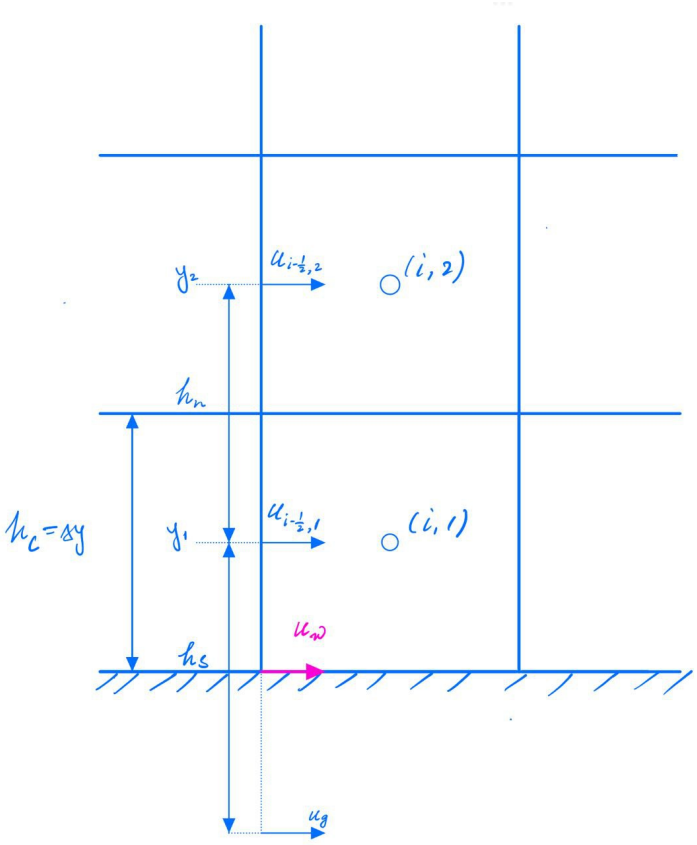

Figure 6: $\hat{L}^u_{yy}$ at the bottom boundary.

It is, in fact, possible to directly use the third velocity directly from the boundary. However, the order of such a scheme will then be reduced due to the large ratio of the distances between the neighbouring velocities. If, on the other hand, we introduce a ghost velocity u_g, we have the freedom of where to place it. Let us use Eq. (8.12) and change the distances between velocities as in Fig. 6, which leads to

$$\left.\frac{\partial^2 u}{\partial y^2}\right|_{i-\frac{1}{2},1} = u_{i-\frac{1}{2},2}\left(\frac{1}{h_n h_c}\right) + u_{i-\frac{1}{2},1}\left(\frac{-2}{h_n h_s}\right) + u_g\left(\frac{1}{h_s h_c}\right). \tag{8.18}$$

The position of u_g is not fixed, we can make the order of the scheme $O(\Delta y^2)$ if $h_s = h_n$. Interpolation of velocity at the wall $u_w = \frac{u_{i-\frac{1}{2},1}+u_g}{2} = 0 \Rightarrow u_g = -2u_{i-\frac{1}{2},1}$, then

$$\begin{aligned}\left.\frac{\partial^2 u}{\partial y^2}\right|_{i-\frac{1}{2},1} &= u_{i-\frac{1}{2},2}\left(\frac{1}{h_n h_c}\right) + u_{i-\frac{1}{2},1}\left(\frac{-2}{h_n h_s} + \frac{-2}{h_s h_c}\right) \\ &= u_{i-\frac{1}{2},2}\left(\frac{1}{h_n h_c}\right) + u_{i-\frac{1}{2},1}\left(\frac{-2h_c - 2h_n}{h_s h_c h_n}\right).\end{aligned} \tag{8.19}$$

The coefficients from Eq. (8.19) are distributed into the $\hat{L}^u_{yy}$ matrix similarly to previous boundary cases.

8.1.5 Right boundary.

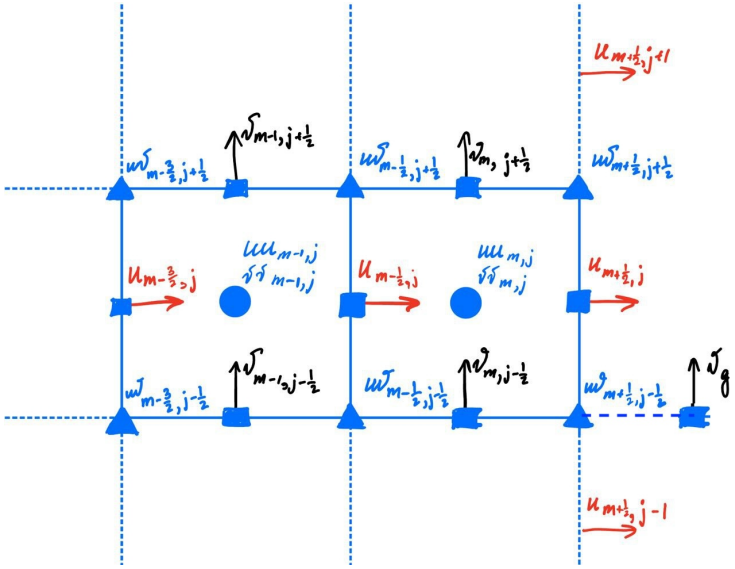

Figure 7: $\hat{L}^u_{xx}, \hat{L}^v_{xx}$ at the right boundary ($m = M$).

INDICATE GHOST VELOCITY POINT

In order to express the rightmost unknown velocity component $u_{M-\frac{1}{2},j}$ inside the domain it is required to use the boundary values of $u_{M+\frac{1}{2},j}$ and ghost elements for v_g as in Fig. 7. The best case scenario would be to have Dirichlet velocity values $\boldsymbol{v}(t, 1, y) \subset \mathbb{R}$ or Neumann boundary condition $\frac{\partial u}{\partial x}\big|_{M+\frac{1}{2},j} = 0$ as in Colonius-Taira [3] at the outlet. However, since the solution of Eqs. (6.1) at the right boundary of the domain might not have the same behaviour, it is not possible to impose such boundary conditions for our problem statement. We will address the spatial discretization of Laplacian at the right boundary in **??**.

8.2 Advection

Since Explicit Adams-Bashforth Eq. (8.3) uses information from time steps n and $n-1$, while we solve the system of equations for time step $n+1$ there is no need for upwinding or even more complicated schemes. For spatial discretization we will try to stick to the central schemes as they are more stable and less dependent on the flow direction. It is convenient to write such schemes for conservative form of the advection, moreover, this also keeps the error low, since there is no product of velocity with acceleration. Hence, let us rewrite advective derivatives in conservative form.

$$\begin{aligned} u\frac{\partial u}{\partial x} + v\frac{\partial u}{\partial y} &= u\frac{\partial u}{\partial x} + 0 + v\frac{\partial u}{\partial y} \\ &= u\frac{\partial u}{\partial x} + u\left(\frac{\partial u}{\partial x} + \frac{\partial v}{\partial y}\right) + v\frac{\partial u}{\partial y} \\ &= \left(u\frac{\partial u}{\partial x} + u\frac{\partial u}{\partial x}\right) + \left(u\frac{\partial v}{\partial y} + v\frac{\partial u}{\partial y}\right) \\ &= \frac{\partial uu}{\partial x} + \frac{\partial uv}{\partial y}. \end{aligned} \tag{8.20}$$

Our goal is to compute advection components at the unknown velocity coordinates. Below we will describe the discretization schemes for Eq. (8.20).

8.2.1 Inner part

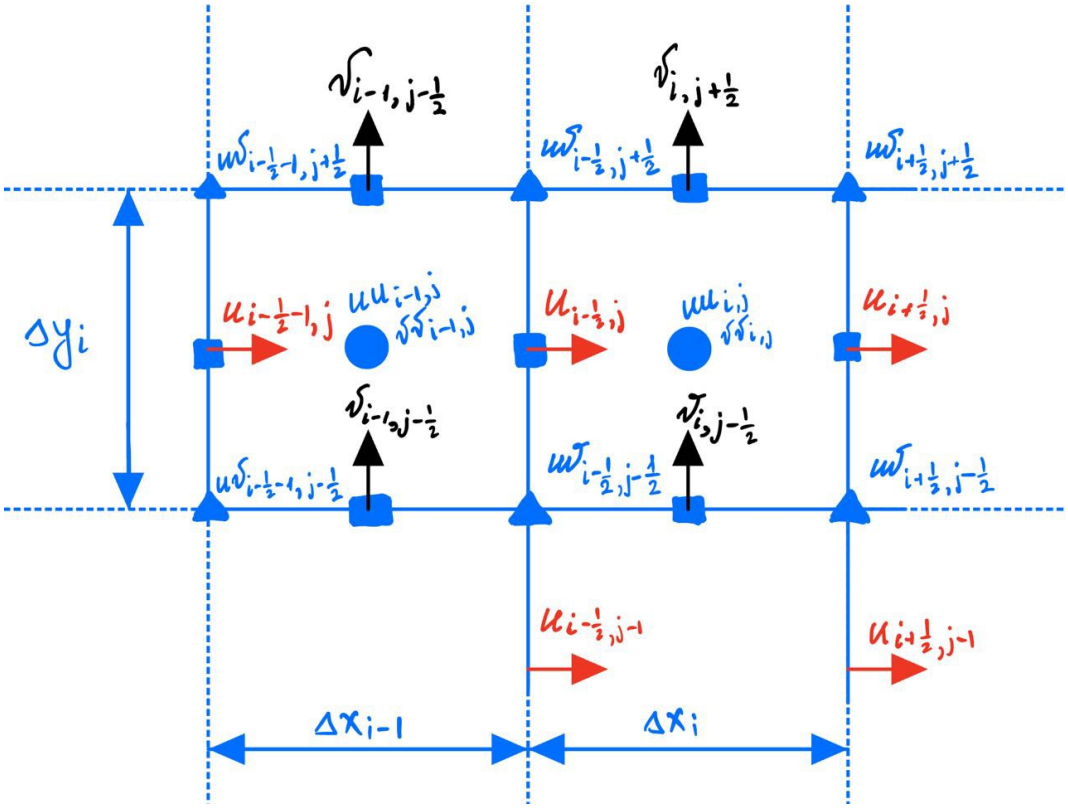

Figure 8: Advection discretization.

Advective component from x-momentum was expressed in conservative form by Eq. (8.20). It is discretized using the standard central differencing schemes [3] as

$$\left(u\frac{\partial u}{\partial x}+v\frac{\partial u}{\partial y}\right)_{i-\frac{1}{2},j}=\frac{(uu)_{i,j}-(uu)_{i-1,j}}{\frac{\Delta x_i+\Delta x_{i-1}}{2}}+\frac{(uv)_{i-\frac{1}{2},j+\frac{1}{2}}-(uv)_{i-\frac{1}{2},j-\frac{1}{2}}}{\Delta y_i}, \tag{8.21}$$

which is evaluated at the same points as $u_{i-\frac{1}{2},j}$ (squares in Fig. 8). We need to compute uv at the nodes and uu at cell centres, which are triangles and circles respectively in Fig. 8. Using linear interpolation [3] of velocity values leads to

$$\begin{aligned}
(uu)_{i,j}&=\left(\frac{u_{i+\frac{1}{2},j}+u_{i-\frac{1}{2},j}}{2}\right)^2,\\
(uv)_{i-\frac{1}{2},j-\frac{1}{2}}&=\left(u_{i-\frac{1}{2},j-1}+\frac{\Delta y_{j-1}}{2}\frac{u_{i-\frac{1}{2},j}-u_{i-\frac{1}{2},j-1}}{\frac{\Delta y_{j-1}+\Delta y_j}{2}}\right)\left(v_{i-1,j-\frac{1}{2}}+\frac{\Delta x_{i-1}}{2}\frac{v_{i,j-\frac{1}{2}}-v_{i-1,j-\frac{1}{2}}}{\frac{\Delta x_{i-1}+\Delta x_i}{2}}\right)\\
&=\left(\frac{u_{i-\frac{1}{2},j}\Delta y_{j-1}+u_{i-\frac{1}{2},j-1}\Delta y_j}{\Delta y_{j-1}+\Delta y_j}\right)\left(\frac{v_{i,j-1\frac{1}{2}}\Delta x_{i-1}+v_{i-1,j-\frac{1}{2}}\Delta x_i}{\Delta x_{i-1}+\Delta x_i}\right).
\end{aligned}$$

8.2.2 Left boundary

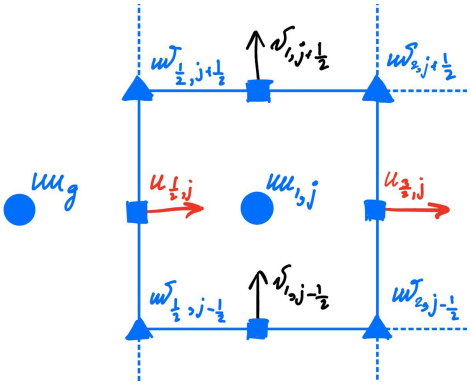

Figure 9: Left boundary advection.

The exact value of the uu_g element located outside the boundary (Fig. 9) is known from the inlet boundary conditions, whereas $uv_{\frac{1}{2},j}$ is zero for all j due to $v_{bc} = 0$ at the inlet.

8.2.3 Top boundary

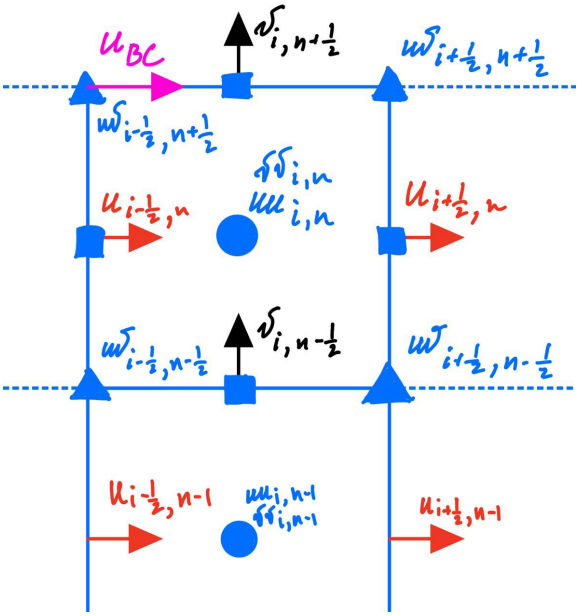

Figure 10: Top boundary advection.

Since the exact values of the velocity u_{BC} and $v_{BC} = 0$ in a freestream are known from **??**, we can directly use them in our advection term computation making the second summand $uv = 0$, in particular

$$\left(\frac{\partial uu}{\partial x} + \frac{\partial uv}{\partial y}\right)_{i-\frac{1}{2},N} = 2\frac{(uu)_{i,N} - (uu)_{i-1,N}}{\Delta x_i + \Delta x_{i-1}} + 0. \tag{8.22}$$

8.2.4 Bottom boundary

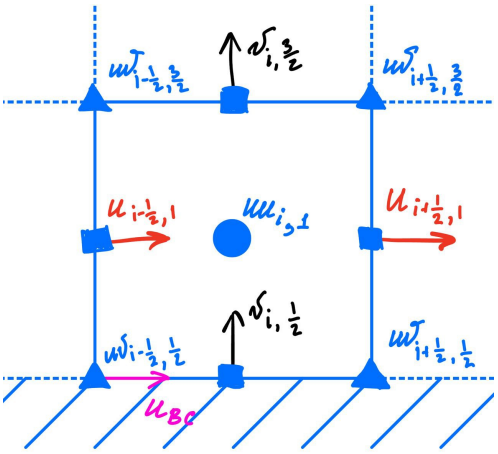

Figure 11: Bottom boundary advection

Computation of the advective terms just above the bottom boundary is the same as for the inner part, with the only exception being $uv_{i-\frac{1}{2},\frac{1}{2}} = 0$ at the boundary, due to the $u_{bc} = 0$ condition on the plate (purple on Fig. 11).

The advective terms in the y-momentum equation are computed similarly. After the derivatives are evaluated, they are moved to the right-hand side as in Sys. (8.5) and treated explicitly.

8.2.5 Right boundary

Similarly to Laplacian for the right side in Section 8.1.5 we need explicit values of u and v at and beyond the boundary. These values are yet to be known, hence, it is not possible to utilize the inner part advection formulas from Section 8.2.1 to rightmost unknown velocities at time steps $n, n-1$ directly. These values are to be determined using artificial boundary conditions in **??**.

8.3 Divergence

One of the advantages of the staggered grid is that the discrete divergence D and gradient G operators are equal to the negative transpose of each other. In this section we will show one side of why this identity is true, the other part could be found in Section 8.4. The second line of Sys. (8.5) reads

$$\begin{aligned}
\hat{D}\boldsymbol{v} &= \hat{bc}_2, \\
\begin{bmatrix} \hat{D}_x & \hat{D}_y \end{bmatrix} \begin{bmatrix} u \\ v \end{bmatrix} &= \hat{bc}_2, \\
\frac{1}{\Delta x} D_x u + \frac{1}{\Delta y} D_y v &= \hat{bc}_2, \\
\frac{1}{\Delta_{xy}} \begin{bmatrix} D_x & D_y \end{bmatrix} \begin{bmatrix} u\Delta y \\ v\Delta x \end{bmatrix} &= \frac{1}{\Delta_{xy}} Dq = \hat{bc}_2,
\end{aligned}$$

where vector $q = \begin{bmatrix} u\Delta y \\ v\Delta x \end{bmatrix}$ is referred to as velocity flux, and the matrix $D = [D_x D_y]$ without hat is the divergence matrix of integer coefficients. Matrix

$$\Delta_{xy} = \begin{bmatrix} \frac{1}{\Delta x_1 \Delta y_1} & 0 & \dots & 0 \\ 0 & \frac{1}{\Delta x_2 \Delta y_1} & \dots & 0 \\ \vdots & \vdots & \ddots & \vdots \\ 0 & 0 & \dots & \frac{1}{\Delta x_M \Delta y_N} \end{bmatrix} \tag{8.23}$$

is $MN \times MN$ diagonal matrix with entries corresponding to the inverse volumes of cells.

The second-order central difference scheme was employed in the construction of D, the order is consistent with the other spatial schemes. Consider a finite volume $V_{i,j}$, continuity equation for the cell centre is then expressed as

$$\left(\frac{\partial u}{\partial x} + \frac{\partial v}{\partial y}\right)_{i,j} = 0,$$

which can be discretized at cell centre i, j using central difference schemes into

$$\frac{u_{i+\frac{1}{2},j} - u_{i-\frac{1}{2},j}}{\Delta x_i} + \frac{v_{i,j+\frac{1}{2}} - v_{i,j-\frac{1}{2}}}{\Delta y_j} = 0.$$

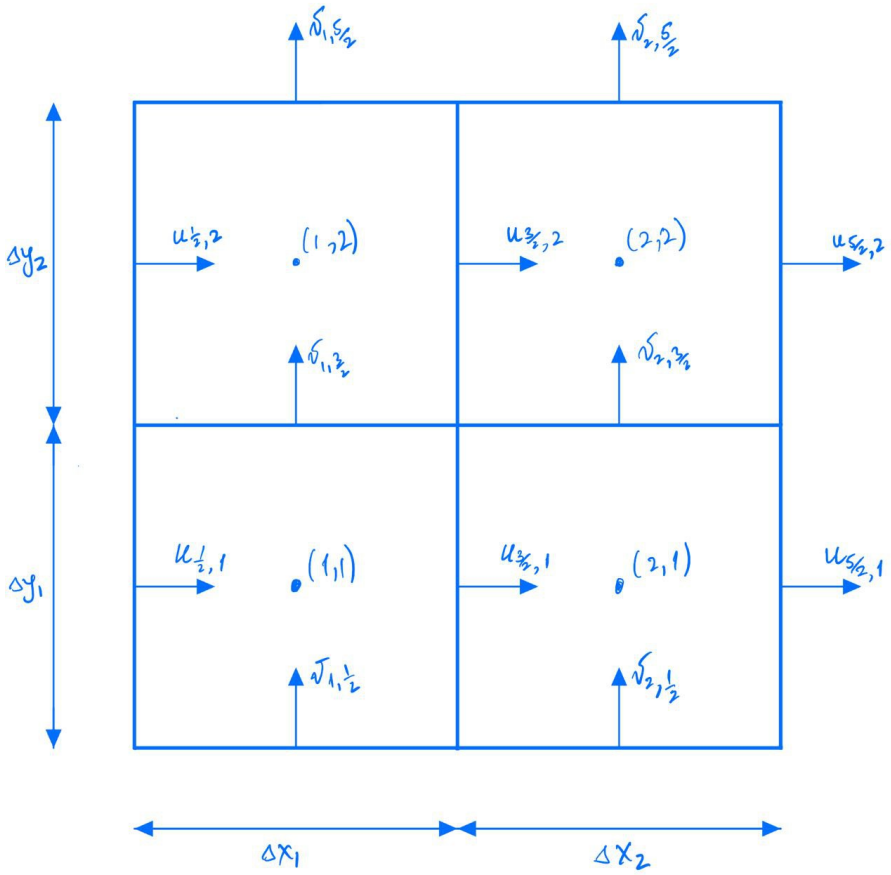

Figure 12: 2×2 grid example for divergence operator.

To provide a good visual example, consider 2×2 grid as in Fig. 12 with the same boundary conditions as in Eqs. (6.1). The partial derivatives of divergence operator evaluated at cell centres are:

$$\begin{aligned}
V_{1,1} &: \frac{u_{\frac{3}{2},1} - u_{\frac{1}{2},1}}{\Delta x_1} + \frac{v_{1,\frac{3}{2}} - v_{1,\frac{1}{2}}}{\Delta y_1} = 0, \\
V_{1,2} &: \frac{u_{\frac{5}{2},1} - u_{\frac{3}{2},1}}{\Delta x_2} + \frac{v_{2,\frac{3}{2}} - v_{2,\frac{1}{2}}}{\Delta y_1} = 0, \\
V_{2,1} &: \frac{u_{\frac{3}{2},2} - u_{\frac{1}{2},2}}{\Delta x_1} + \frac{v_{1,\frac{5}{2}} - v_{1,\frac{3}{2}}}{\Delta y_2} = 0, \\
V_{2,2} &: \frac{u_{\frac{5}{2},2} - u_{\frac{3}{2},2}}{\Delta x_2} + \frac{v_{2,\frac{5}{2}} - v_{2,\frac{3}{2}}}{\Delta y_2} = 0.
\end{aligned}$$

16 After applying the boundary conditions (circled on the figure 7) to the above equations, we obtain the system

$$\begin{bmatrix} \frac{1}{\Delta x_1 \Delta y_1} & 0 & 0 & 0 \\ 0 & \frac{1}{\Delta x_2 \Delta y_1} & 0 & 0 \\ 0 & 0 & \frac{1}{\Delta x_1 \Delta y_2} & 0 \\ 0 & 0 & 0 & \frac{1}{\Delta x_2 \Delta y_2} \end{bmatrix} \begin{bmatrix} 1 & 0 & 0 & 0 & 1 & 0 \\ -1 & 1 & 0 & 0 & 0 & 1 \\ 0 & 0 & 1 & 0 & -1 & 0 \\ 0 & 0 & -1 & 1 & 0 & -1 \end{bmatrix} \begin{bmatrix} u_{\frac{3}{2},1}\Delta y_1 \\ u_{\frac{5}{2},1}\Delta y_1 \\ u_{\frac{3}{2},2}\Delta y_2 \\ u_{\frac{5}{2},2}\Delta y_2 \\ v_{1,\frac{3}{2}}\Delta x_1 \\ v_{2,\frac{3}{2}}\Delta x_2 \end{bmatrix} = \begin{bmatrix} \frac{u_{\frac{1}{2},1}}{\Delta x_1} + \frac{v_{1,\frac{1}{2}}}{\Delta y_1} \\ \frac{v_{2,\frac{1}{2}}}{\Delta y_1} \\ \frac{u_{\frac{1}{2},2}}{\Delta x_1} - \frac{v_{1,\frac{5}{2}}}{\Delta y_2} \\ -\frac{v_{2,\frac{5}{2}}}{\Delta y_2} \end{bmatrix}, \tag{8.24}$$

which in general case is written as $\frac{1}{\Delta_{xy}} Dq = \hat{bc}_2$. The velocity values known at the boundaries are shifted to the right-hand side and explicitly treated. The divergence matrix D contains ± 1, as shown in Sys. (8.24).

8.4 Gradient

The pressure gradients are computed at the same coordinates as the unknown velocities according to Sys. (8.1). Below we will show that the discrete gradient and divergence operators satisfy

$$G = -D^T \tag{8.25}$$

on staggered/MAC grids by construction.

As an illustrative example, we may consider a 2×2 grid as in Fig. 13 with the same boundary conditions as in Eqs. (6.1). It is required to determine the pressure gradients across each unknown velocity (square nodes on Fig. 13):

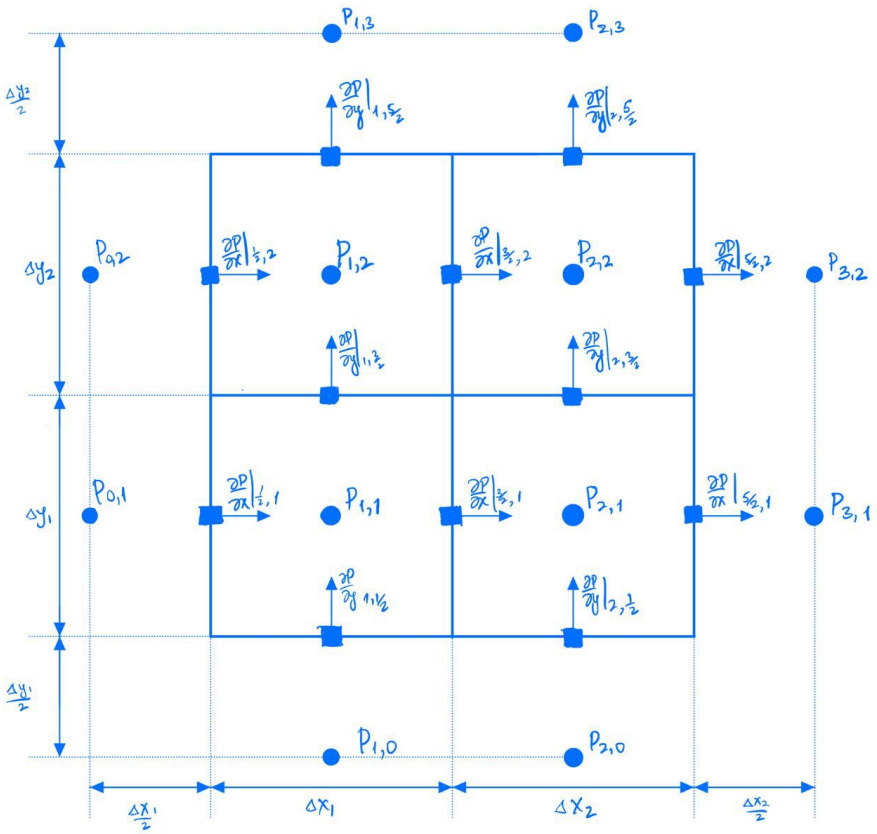

Figure 13: 2×2 grid example for gradient operator.

$$
\begin{aligned}
u_{1,2} &: \frac{2}{\Delta x_1 + \Delta x_2}\left(p_{2,1} - p_{1,1}\right), \\
u_{1,3} &: \frac{1}{\Delta x_2}\left(p_{3,1} - p_{2,1}\right), \\
u_{2,2} &: \frac{2}{\Delta x_1 + \Delta x_2}\left(p_{2,2} - p_{1,2}\right), \\
u_{2,3} &: \frac{1}{\Delta x_2}\left(p_{3,2} - p_{2,2}\right), \\
v_{2,1} &: \frac{2}{\Delta y_1 + \Delta y_2}\left(p_{1,2} - p_{1,1}\right), \\
v_{2,2} &: \frac{2}{\Delta y_1 + \Delta y_2}\left(p_{2,2} - p_{2,1}\right).
\end{aligned}
$$

The next step is to rewrite the above expressions in matrix form using the pressure boundary conditions outside the grid. The resultant system of linear equations then becomes

$$
\begin{bmatrix}
\frac{2}{\Delta x_1+\Delta x_2} & 0 & 0 & 0 & 0 & 0 \\
0 & \frac{1}{\Delta x_2} & 0 & 0 & 0 & 0 \\
0 & 0 & \frac{2}{\Delta x_1+\Delta x_2} & 0 & 0 & 0 \\
0 & 0 & 0 & \frac{1}{\Delta x_2} & 0 & 0 \\
0 & 0 & 0 & 0 & \frac{2}{\Delta y_1+\Delta y_2} & 0 \\
0 & 0 & 0 & 0 & 0 & \frac{2}{\Delta y_1+\Delta y_2}
\end{bmatrix}
\left(
\begin{bmatrix}
-1 & 1 & 0 & 0 \\
0 & -1 & 0 & 0 \\
0 & 0 & -1 & 1 \\
0 & 0 & 0 & -1 \\
-1 & 0 & 1 & 0 \\
0 & -1 & 0 & 1
\end{bmatrix}
\begin{bmatrix} p_{1,1} \\ p_{2,1} \\ p_{1,2} \\ p_{2,2} \end{bmatrix}
+
\begin{bmatrix} 0 \\ p_{3,1} \\ 0 \\ p_{3,2} \\ 0 \\ 0 \end{bmatrix}
\right),
\tag{8.26}
$$

which can be written in compact format as

$$
\nabla p + bc_p \Longleftrightarrow \Delta_{xy}\left(\hat{G}\begin{bmatrix} p_{1,1} \\ p_{1,2} \\ \vdots \\ p_{mn+(n-1)m} \end{bmatrix} + bc_p\right)
$$

where $\hat{M}^{-1}$ is the diagonal matrix containing the distances between neighbouring pressure coordinates, G is the gradient matrix and $[p_1, p_2, ..., p_{mn+(n-1)m}]^T$ is the vector of pressure values at the cell centres. There are some pressure BC values in bc_p since there is a pressure gradient that has to be computed across the boundary. It can be observed from Sys. (8.24) and (8.26) that Eq. (8.25) holds and the general case is true by construction.

9 Normalization

The most effective methods for solving systems of linear equations often work optimally with symmetric matrices, making symmetry a desirable property. In order to achieve a symmetric system, we introduce two matrices - the diagonal scaling matrix $\hat{M}$ and the diagonal flux matrix R. These matrices are defined as

$$R \equiv \begin{bmatrix} \Delta y_j & 0 \\ 0 & \Delta x_i \end{bmatrix},$$
$$\hat{M} \equiv \begin{bmatrix} \frac{1}{2}(\Delta x_i + \Delta x_{i-1}) & 0 \\ 0 & \frac{1}{2}(\Delta y_j + \Delta y_{j-1}) \end{bmatrix}.$$

Define matrices

$$\Delta y_j = \mathrm{diag}([\underbrace{\Delta y_1; \Delta y_1; \dots; \Delta y_1}_{M-1 \text{ times}}; \underbrace{\Delta y_2; \Delta y_2; \dots; \Delta y_2}_{M-1 \text{ times}}; \dots; \underbrace{\Delta y_N; \Delta y_N; \dots; \Delta y_N}_{M-1 \text{ times}}]),$$
$$\Delta x_i = \mathrm{diag}([\underbrace{\Delta x_1; \Delta x_2; \dots \Delta x_M; \Delta x_1; \Delta x_2; \dots \Delta x_M; \dots; \Delta x_1; \Delta x_2; \dots; \Delta x_M}_{N-1 \text{ blocks of } 1,\dots,M}]),$$

which are then combined into

$$R = \begin{bmatrix} \Delta y_j & 0 \\ 0 & \Delta x_i \end{bmatrix}.$$

By moving to new variable $q = R\boldsymbol{v}$, we use matrix R, which inverse R^{-1} performs half of the symmetrization process for $\hat{L}$. Here, R is a diagonal matrix of size $(M-1)N \times M(N-1)$. Using the R matrix we can express mass flux $q^{n+1} = R\boldsymbol{v}^{n+1} \implies \boldsymbol{v}^{n+1} = R^{-1}q^{n+1}$. It is required that the difference matrices cancel out $\frac{x_{i+1}-x_{i-1}}{2}$ central term in diffusion discretization to make Laplacian partially symmetric. Define the elements of diagonal mass matrix as

$$\Delta x_i + \Delta x_{i-1} = \mathrm{diag}[\underbrace{\Delta x_2 + \Delta x_1; \Delta x_3 + \Delta x_2; \dots; \Delta x_M + \Delta x_{M-1}; \dots; \Delta x_2 + \Delta x_1; \Delta x_3 + \Delta x_2; \dots \Delta x_M + \Delta x_M}_{N \text{ times for each block of } \Delta x_2+\Delta x_1 \text{ to } \Delta x_M+\Delta x_{M-1}}]$$

and

$$\Delta y_j + \Delta y_{j-1} = \mathrm{diag}[\underbrace{\Delta y_2 + \Delta y_1; \dots \Delta y_2 + \Delta y_1}_{M \text{ times}}; \underbrace{\Delta y_3 + \Delta y_2; \dots \Delta y_3 + \Delta y_2}_{M \text{ times}}; \underbrace{\Delta y_N + \Delta y_{N-1} \dots \Delta y_N + \Delta y_{N-1}}_{M \text{ times}}],$$

which are then combined into

$$\hat{M} = \begin{bmatrix} \frac{1}{2}(\Delta x_i + \Delta x_{i-1}) & 0 \\ 0 & \frac{1}{2}(\Delta y_j + \Delta y_{j-1}) \end{bmatrix},$$

which both removes the M^{-1} in $\hat{G} = \hat{M}^{-1}G$ if left multiplied and completes the symmetrization process of $\hat{L}$.

The identity $q = R\boldsymbol{v}$ implies $\boldsymbol{v} = R^{-1}q$, therefore, Laplacian matrix multiplied by the velocity vector is

$$\hat{L}\boldsymbol{v} = \hat{L}R^{-1}q,$$

premultiplying by $\hat{M}$ we obtain

$$\hat{M}\hat{L}R^{-1}q,$$

where $\hat{M}LR^{-1}$ is symmetric by construction, hence, $\hat{M}\hat{A}R^{-1} = \hat{M}(\frac{1}{\Delta t}\mathbf{I} - \frac{1}{2}L)R^{-1}$ is also symmetric.

Using the above transformations we can modify Sys. (8.8) into

$$\begin{bmatrix} \hat{M}\hat{A}R^{-1} & \hat{M}\hat{G} \\ \hat{D}R^{-1} & 0 \end{bmatrix} \begin{pmatrix} q^{n+1} \\ p^{n+1} \end{pmatrix} = \begin{pmatrix} \hat{M}\hat{r}^n \\ 0 \end{pmatrix} + \begin{pmatrix} \hat{M}\widehat{bc}_1 \\ \widehat{bc}_2 \end{pmatrix},$$

which can be rewritten as

$$\boxed{\begin{bmatrix} A & G \\ D & 0 \end{bmatrix} \begin{pmatrix} q^{n+1} \\ p^{n+1} \end{pmatrix} = \begin{pmatrix} r^n \\ 0 \end{pmatrix} + \begin{pmatrix} bc_1 \\ bc_2 \end{pmatrix},} \tag{9.1}$$

where $A = \hat{M}\hat{A}R^{-1} = \frac{1}{\Delta t}\hat{M}R^{-1} - \frac{1}{2}\hat{M}\hat{L}R^{-1}$ is symmetric and $\hat{G} = \hat{M}^{-1}G$ according to Sys. (8.26). It is also possible to transform the divergence operator $\hat{D}$ with non-integer coefficients into D with integer coefficients in continuity part of Sys. (9.1) using Sys. (8.24). Multiplying both sides of continuity equation by Δ_{xy} matrix from Eq. (8.23) leads to

$$\begin{aligned}
\hat{D}\boldsymbol{v}^{n+1} &= \hat{bc}_2 \\
(\Delta_{xy})\,\hat{D}\boldsymbol{v}^{n+1} &= (\Delta_{xy})\,\hat{bc}_2 \\
(\Delta_{xy})\,\frac{1}{\Delta_{xy}}DR\boldsymbol{v}^{n+1} &= (\Delta_{xy})\,\hat{bc}_2 \\
(\Delta_{xy})\,\frac{1}{\Delta_{xy}}Dq^{n+1} &= (\Delta_{xy})\,\hat{bc}_2 \\
Dq^{n+1} &= bc_2.
\end{aligned}$$

10 Nullspace method and pressure elimination in terms of discrete operators

The goal of this subsection is to show how unknown pressure variables can be eliminated from Sys. (9.1) similarly to Section 2. Publications of Chang [2] and Hall [5] use the idea that in Sys. (9.1) matrix D is wider than tall for grids larger than 2×2, hence it defines a nullspace. The nullspace of matrix D is the set of all solutions to the homogeneous linear system $Dx = 0$, where x is a vector in the null space of D. Let C be the nullspace matrix containing such vectors x.

The number of rows in the nullspace C is equal to the number of faces with unknown velocities (N_f). In two dimensions C has N_n columns, which is equal to the number of nodes in the grid, whereas in three dimensions the nullspace has N_e columns being the number of edges.

In the two-dimensional case, the matrix C has two non-zero elements in each row, which are $+1$ and -1. The $+1$ value corresponds to the node $90°$ from the normal velocity vector, whereas -1 corresponds to the node $-90°$ from the normal velocity vector. For three dimensional case see Chang [2].

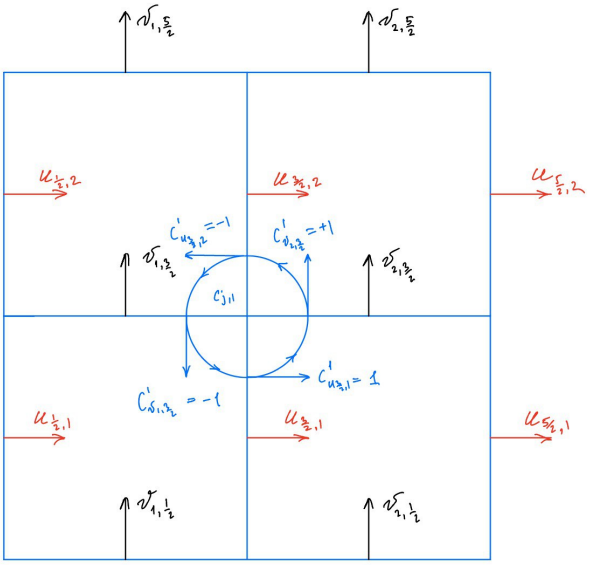

Figure 14: 2×2 example for C matrix.

A more intuitive way of constructing the matrix C relies on the utilization of counterclockwise vorticity around the nodes within the domain (Fig. 14). If the direction of the velocity vector on the adjacent face aligns with the vorticity's direction, +1 is assigned to the corresponding row; conversely, -1 is assigned in the case of opposite directions of velocity and vorticity. After applying the above procedure we obtain

$$C = \begin{bmatrix} 1 \\ -1 \\ -1 \\ 1 \end{bmatrix}.$$

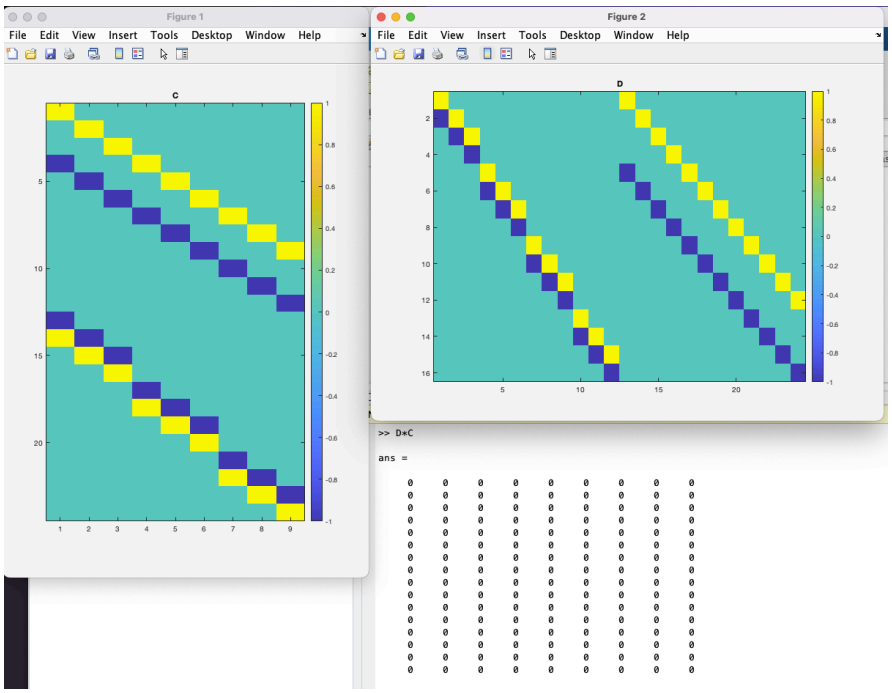

Figure 15: Divergence and Curl matrices.

The matrix C has dimensions corresponding to unknown velocities times the number of nodes around which these velocities revolve. Figure 15 illustrates matrices D and C for a 4×4 grid with an open boundary on the right side of the domain. The desired product then becomes $DC = 0$. $D = -G^T$ (derived in Sections 8.3 and 8.4) leads to important property $(DC)^T = C^T D^T = -C^T G = 0$. Premultiplying momentum equation in Sys. (9.1) by C^T creates $C^T G p = 0$ term, which completely eliminates the pressure from our system.

In order to make use of efficient solvers, the matrix $C^T A$ can be made symmetric if multiplied by C from the right. We use the property of product $C^T C = -L$ being symmetric Laplacian and $C^T L C = -L^2$ being symmetric biharmonic operator as in Eq. (3.9). Matrix $C^T C = -L^2$ has zero boundary conditions for the vector it is applied to. Hence, the final chord of this method is the introduction of new variable called discrete streamfunction $\psi : q_h = C\psi$, where q_h is a homogeneous solution to the Sys. (9.1) and $q = q_h + q_p$ decomposition is discussed in the following Section 11.

11 Resulting algorithm

Let us consider the solution to discretized Sys. (9.1)

$$q^{n+1} = q_p^{n+1} + q_h^{n+1},$$

where q_h^{n+1} is a solution of homogeneous continuity equation

$$Dq_h^{n+1} = 0, \tag{11.1}$$

and q_p^{n+1} is a particular solution to a non-homogeneous continuity equation

$$Dq_p^{n+1} = bc_2. \tag{11.2}$$

We assume that momentum equation from Sys. (9.1) is modified to streamfunction Eq. (3.9) with biharmonic operator satisfies homogeneous Eq. (11.1) as in Colonius-Taira [3]. The difference between [3] and the method described below lies in boundary conditions. Colonius and Taira used homogeneous conditions at all boundaries (e.g. $\frac{\partial u}{\partial x} = 0$ at inlet-outlet). Therefore, it was not needed for them to solve an additional non-homogeneous Eq. (11.2), whereas, in our problem statement such equation has to be solved due to non-zero Dirichlet and Neumann boundary conditions.

Taking into account continuous operator identities in Section 3, the resulting algorithm for discrete Navier-Stokes Sys. (9.1) can be described as follows:

1. Construct curl matrix C, such that $DC = 0$ and $q_h = C\psi$.
2. Rewrite $q^{n+1} = q_p^{n+1} + q_h^{n+1}$.
3. Find q_p^{n+1} from the non-homogeneous continuity Eq. (11.2) using the method described in next Section 12.
4. Split the solution q^{n+1} into homogeneous and particular, then eliminate the pressure terms in the momentum equation.

$$\begin{aligned}
Aq^{n+1} &= -Gp^{n+1} + bc_1, && \\
A(q_h^{n+1} + q_p^{n+1}) &= D^T p^{n+1} + bc_1, && \text{premultiply by } C^T, \\
C^T A q_h^{n+1} &= C^T(bc_1 - Aq_p^{n+1}), && \text{use } q_h^{n+1} = C\psi^{n+1}, \\
C^T AC\psi^{n+1} &= C^T(bc_1 - Aq_p^{n+1}). &&
\end{aligned} \tag{11.3}$$

   The above Sys. (11.3) is solving Eq. (3.9) using Euler scheme $\frac{\partial \psi}{\partial t} = \frac{\psi^{n+1} - \psi^n}{\Delta t}$.
5. Solve resulting Sys. (11.3) for ψ^{n+1}.
6. Obtain $q_h^{n+1} = C\psi^{n+1}$.
7. Compute $q^{n+1} = q_p^{n+1} + q_h^{n+1}$ and convert it to velocity vector field $\boldsymbol{v}^{n+1} = R^{-1}q^{n+1}$.
8. Transition to the next time instance by repeating Steps (3) to (7) using the new boundary values from q^{n+1}.

Steps (3) and (7) and changing values at the boundary of Step (8) were not necessary in Colonius-Taira [3], whereas Step (2) used homogeneous property $bc_2 = 0$ of continuity Eq. (11.2), making $q^{n+1} = q_h^{n+1}$.

12 Particular solution using Lagrange multipliers

It is possible to find one particular solution to the discrete non-homogeneous continuity Eq. (11.2) using the method of Lagrange multipliers as follows

$$Dq_p^{n+1} = bc_2, \implies \mathcal{L}(q_p, \lambda) = \|q_p\|^2 + \lambda^T (bc_2 - Dq_p). \tag{12.1}$$

Differentiating w.r.t q_p and finding the minimum (derivative equal to zero) yields to

$$2q_p - D^T\lambda = 0. \tag{12.2}$$

We may premultiply by D to obtain

$$2Dq_p - DD^T\lambda = 0,$$

then the substitution of $bc_2 = Dq_p$ will lead to

$$\begin{aligned} 2bc_2 &= DD^T\lambda, \\ \lambda &= 2\left(DD^T\right)^{-1} bc_2, \end{aligned}$$

plugging the above into Eq. (12.2) results in

$$q_p = D^T\left(DD^T\right)^{-1} bc_2 = D^\dagger bc_2,$$

where $D^\dagger = D^T\left(DD^T\right)^{-1}$ is called pseudo-inverse. In the method above we minimize the square of the mass flux, which is equivalent to the minimization of kinetic energy.

13 Summary

References

[1] MATH 248: Honours Vector Calculus Fall 2019. https://www.math.mcgill.ca/gantumur/math248f19/.

[2] Wang Chang, Francis Giraldo, and Blair Perot. Analysis of an exact fractional step method. *Journal of Computational Physics*, 180(1):183–199, 2002.

[3] Tim Colonius and Kunihiko Taira. A fast immersed boundary method using a nullspace approach and multi-domain far-field boundary conditions. *Computer Methods in Applied Mechanics and Engineering*, 197:2131–2146, April 2008.

[4] Björn Engquist and Andrew Majda. Absorbing boundary conditions for numerical simulation of waves. *Proceedings of the National Academy of Sciences*, 74(5):1765–1766, May 1977.

[5] C. Hall, T. Porsching, R. Dougall, R. Amit, A. Cha, C. Cullen, George Mesina, and Samir Moujaes. Numerical methods for thermally expandable two-phase flow-computational techniques for steam generator modeling. *NASA STI/Recon Technical Report N*, 1980.

[6] F. Harlow and E. Welch. Numerical calculation of time-dependent viscous incompressible flow of fluid with free surface. *Physics of Fluids*, 8:2182–2189, 1965.

[7] G. Jin and M. Braza. A Nonreflecting Outlet Boundary Condition for Incompressible Unsteady Navier-Stokes Calculations. *Journal of Computational Physics*, 107(2):239–253, August 1993.

[8] A. Kourta, M. Braza, P. Chassaing, and H. Haminh. Numerical analysis of a natural and excited two-dimensional mixing layer. *AIAA Journal*, 25(2):279–286, February 1987.

[9] C. Liu and Z. Liu. High Order Finite Difference and Multigrid Methods for Spatially Evolving Instability in a Planar Channel. *Journal of Computational Physics*, 106(1):92–100, May 1993.

[10] Hélène Persillon and Marianna Braza. Physical analysis of the transition to turbulence in the wake of a circular cylinder by three-dimensional Navier–Stokes simulation. *Journal of Fluid Mechanics*, 365:23–88, June 1998.

[11] R. L. Sani and P. M. Gresho. Résumé and remarks on the open boundary condition minisymposium. *International Journal for Numerical Methods in Fluids*, 18(10):983–1008, 1994.

[12] Semyon V. Tsynkov. Numerical solution of problems on unbounded domains. A review. *Applied Numerical Mathematics*, 27(4):465–532, August 1998.

[13] O. Zikanov. *Essential Computational Fluid Dynamics*. Wiley, Hoboken, N.J., 2010.

A Appendix

A.1 Transient schemes